



The effect of annealing time in oxygen flux on the electric properties of the $\text{Ru}(\text{Sr}_{2-x}\text{Ca}_x)\text{GdCu}_2\text{O}_{8\pm z}$ system with $0.0 < x < 2.0$, prepared at ambient pressure

M. Abatal ^a, E. Chavira ^{a,*}, C. Filippini ^b, V. García-Vázquez ^c,
J.C. Pérez ^c, J.L. Tholence ^b, H. Noël ^d

^a IIM-UNAM, AP 70-360, 04510 México D.F., Mexico

^b LEPES-CNRS, 25 Ave. des Martyrs, BP 166, 38048 Grenoble, France

^c IF-LRT, BUAP, AP J-48, 72570 Puebla, Pue., Mexico

^d LCSIM, Ave. Général Leclerc, 35042 Renne, France

Received 9 September 2004; received in revised form 14 April 2005; accepted 20 April 2005

Abstract

A solid-state reaction method for synthesis of $\text{Ru}(\text{Sr}_{2-x}\text{Ca}_x)\text{GdCu}_2\text{O}_{8\pm z}$ system within the composition range of $0.0 < x < 2.0$, at ambient pressure and within the range of 960–1070 °C is reported. The temperature interval for the preparation of the solid solution is determined by differential thermal analysis (DTA) in air. A solid solution is shown to exist up to $x = 0.1$, with a crystalline structure that is isomorphous to $\text{RuSr}_2\text{GdCu}_2\text{O}_8$ (Ru-1212) compound observed by X-ray powder diffraction (XRD). The studies by the scanning electron microscopy (SEM) technique gives a particle size around 1–6 μm . The results of transmission electron microscopy (TEM) studies confirm the tetragonal unit cell of $\text{Ru}(\text{Sr}_{2-x}\text{Ca}_x)\text{GdCu}_2\text{O}_{8\pm z}$ system. The temperature dependence of the electrical resistivity of the samples annealed in oxygen flux for 12 and 41 h, respectively at $T = 960$ °C shows a semiconductor behavior.

© 2005 Elsevier B.V. All rights reserved.

Keywords: Synthesis; XRD; SEM; TEM; Electric resistivity

1. Introduction

The copper–ruthenium oxides $\text{RuSr}_2\text{LnCu}_2\text{O}_8$ and $\text{RuSr}_2(\text{Ln}_{1+x}\text{Ce}_x)\text{Cu}_2\text{O}_{10}$ with Ln = Sm, Eu and Gd were synthesized for the first time by Bauernfeind et al. [1,2]. Most recent experimental

* Corresponding author. Tel.: +52 55 56 22 46 29; fax: +52 55 56 16 12 51.

E-mail address: chavira@servidor.unam.mx (E. Chavira).

and theoretical investigations have focused on studying the coexistence of ferromagnetism and superconductivity in these systems. The Ru-1212 layered cuprate exhibits a unit cell very similar to the $\text{YBa}_2\text{Cu}_3\text{O}_7$ system; the Ru ions replace the Cu ions in the chain-sites, thus giving alternatively CuO_2 bilayers and RuO_2 monolayers [3]. In general, the results of different substitutions on the physical properties in the ruthenocuprate have been reported in the literature [4–10]. The $\text{RuSr}_2\text{LnCu}_2\text{O}_8$ system, with Ln = Sm, Eu and Gd shows that the ferromagnetic order appears at a rather higher Curie temperature between 120 and 150 K, whereas superconductivity occurs at a significantly lower temperatures, $T_c = 10\text{--}40$ K. A similar phenomenon was also observed in the $\text{RuSr}_2(\text{Gd}_{1.5}\text{Ce}_{0.5})\text{Cu}_2\text{O}_{10}$ compound [4]. The physical properties of ruthenocuprate materials are strongly dependent on the preparation conditions [5]. The La ion substitution on the Sr ion site and Ta, Nb, Ti ions in the Ru ion site leads to the suppression of superconductivity in the Ru-1212 compound [11,12]. Yang et al. [10] have reported an increase in superconducting transition temperature by substitution of Ba for Sr in $\text{Ru}(\text{Sr}_{2-x}\text{Ba}_x)\text{GdCu}_2\text{O}_8$ system, with $0 \leq x \leq 0.1$, synthesized by solid-state reaction at ambient pressure. The substitution of Sr^{2+} by Ba^{2+} ions did not change the ferromagnetic transition temperature ($T_M = 136$ K) as found using AC and DC magnetic measurements. In this paper the synthesis of the $\text{Ru}(\text{Sr}_{2-x}\text{Ca}_x)\text{GdCu}_2\text{O}_8$ system with $0.0 < x < 2.0$, by solid-state reaction at ambient pressure is reported using temperatures as high as 1070°C . The results of XRD, SEM, TEM analysis and the measurements of their electric and magnetic properties are also exhibited.

2. Experimental

2.1. Synthesis

The $\text{Ru}(\text{Sr}_{2-x}\text{Ca}_x)\text{GdCu}_2\text{O}_z$ system with $x = 0.0, 0.05, 0.1, 0.2, 0.5$ and 2.0 was synthesized by the solid-state reaction technique at ambient pressure. The starting materials were: RuO_2 anhydrous (99.9% STREM), Gd_2O_3 (99.99%, STREM), CuO

(99.99%, ALDRICH), SrCO_3 (99.5%, CERAC) and CaCO_3 (99.99%, BAKER). Prior to weighing, SrCO_3 and CaCO_3 were preheated for 10–20 min at 120°C dehydration. RuO_2 was weighed in an argon flowing glove bag to avoid the decomposition of this reagent. A stoichiometric mixture of these compounds was ground in an agate mortar in air. The reactions were carried out in an electric furnace ($\pm 4^\circ\text{C}$) between 960 and 1070°C , in air, for 17–94 h in platinum crucibles with intermediate grindings. The resulting powders with $0.0 < x < 0.2$ were pressed into pellets and annealed at a rate of $50^\circ\text{C min}^{-1}$ in a flow of oxygen at 960°C for 12 and 41 h, then slowly cooled to room temperature with a ramp of $30^\circ\text{C min}^{-1}$.

2.2. Characterization

In order to determine the temperature interval in which the reaction should be carried out, DTA experiments were performed using Modulated DSC 9210, TA instruments. The polycrystalline samples were placed in platinum crucibles and heated from ambient temperature up to 1200°C with heating rates of $10^\circ\text{C min}^{-1}$ in air.

XRD patterns were obtained on a SIEMENS D5000 diffractometer using $\text{Cu K}\alpha_1$ radiation. Diffraction patterns were collected at room temperature over the 2θ range $10\text{--}80^\circ$ with a step size of 0.02° and time per step of 10 s. The cell parameters a and c are calculated considering, respectively, the reflections (200) and (005). Refinement of crystal structures was carried out using the Rietveld method with the FullProf program [13]. The first step involved the refinement of the scale factor, the “zero” of the counter, background parameters, cell parameters and profile parameters. In the second step were refined the position parameters, the site occupancies p and the isotropic thermal parameters B (\AA^2).

SEM and electron dispersive X-ray (EDX) were performed on a Leica-Cambridge Stereoscan 400, equipped with an Oxford/Link System electron probe microanalyzer (EPMA). The micrographs were taken with 5.00 K.X, voltage of 20 kV, current intensity of 1000 pA and $\text{WD} = 25$ mm.

The crystal structure of the $\text{Ru}(\text{Sr}_{2-x}\text{Ca}_x)\text{GdCu}_2\text{O}_8$ system was studied by TEM with a

JEM-1200EXII microscope. The diffraction patterns were taken with a voltage of 120 KV and a current intensity of 70–80 μA , the distance of the chamber being 100 cm.

The standard four-probe method with DC resistance measurements was used as a function of temperature. The system is made up in a close-cycle refrigerator tool with conventional equipment for low-level electrical measurements. Continuous monitoring of all electrical parameters during a measurement cycle allows systematic errors in the resistance values to be detected in real-time, permitting clean R vs. T profiles to be obtained with no need of additional mathematical treatment to the experimental data [14]. The DC magnetic measurements were performed using a superconducting quantum interference device (SQUID) Quantum Design MPMS.

3. Results and discussion

DTA results show several endothermic transitions in the temperature ranges: $T = 655\text{--}738$ $^{\circ}\text{C}$ that corresponds to the oxisals decomposition and beginning of some reactions, $T = 894\text{--}985$ $^{\circ}\text{C}$ which we attributed to the formation of different compounds and $T = 1217\text{--}1350$ $^{\circ}\text{C}$ that was related to the fusion of the material. When $x = 0.5$ we noted an exothermic transitions around $958\text{--}995$ $^{\circ}\text{C}$ that it was correlated to creation of some phases observed by XRD.

The XRD patterns of $\text{Ru}(\text{Sr}_{2-x}\text{Ca}_x)\text{GdCu}_2\text{O}_8$ system, with $x = 0.0, 0.05, 0.1$ and 0.2 , show a solubility up to $x = 0.1$ (Fig. 1). The sample with $x = 0.2$ shows reflections of a secondary phase (identified as $\text{Sr}_2\text{GdRuO}_6$ and SrRuO_3). For the sample with $x = 0.5$ the following compounds were obtained: $\text{Sr}_2\text{GdRuO}_6$, CaCu_2O_2 and Ru-1212 (Fig. 2) at 1045 $^{\circ}\text{C}$ in air for 17 h. For the sample with $x = 2.0$ a mixture of CaCu_2O_3 , Gd_3Ru and Ru-1212 compounds was observed (Fig. 3) at 1070 $^{\circ}\text{C}$ in air for 48 h. The XRD diffractograms were analyzed on the basis of the reported tetragonal unit cell [8,9] with a space group P4/mmm that was used to index the patterns. In Fig. 4 we present the Rietveld results of $\text{Ru}(\text{Sr}_{1.9}\text{Ca}_{0.1})\text{GdCu}_2\text{O}_8$ composition.

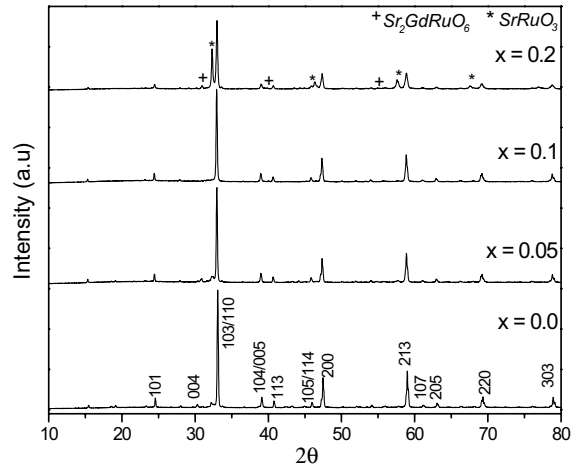


Fig. 1. XRD patterns of $\text{Ru}(\text{Sr}_{2-x}\text{Ca}_x)\text{GdCu}_2\text{O}_8$ system.

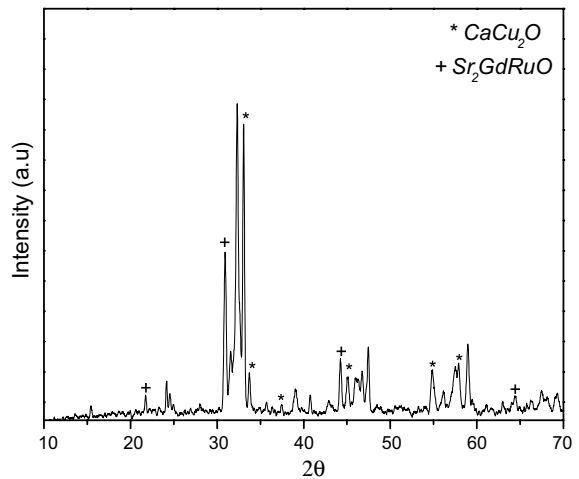


Fig. 2. XRD for $\text{Ru}(\text{Sr}_{1.5}\text{Ca}_{0.5})\text{GdCu}_2\text{O}_8$ compound.

The variation of the lattice parameters a and c with Ca content (x) of the samples, with the composition range of $0.0 < x < 0.2$, annealing in air, is given in Fig. 5. Both a and c decrease with an increasing Ca content (x) since the ionic ratio of Ca^{2+} ion is lower than that of the Sr^{2+} ion (ionic radii $(\text{IR})^{\text{XII}} \text{Ca}^{2+} = 1.34$ \AA and $\text{IR}^{\text{XII}} \text{Sr}^{2+} = 1.44$ \AA) [15] and indicate that Ca ions are successfully substituted for Sr ions.

Particle size and morphology of the samples were studied by SEM analyses. In Fig. 6, the micrograph of $\text{Ru}(\text{Sr}_{1.9}\text{Ca}_{0.1})\text{GdCu}_2\text{O}_8$ compound

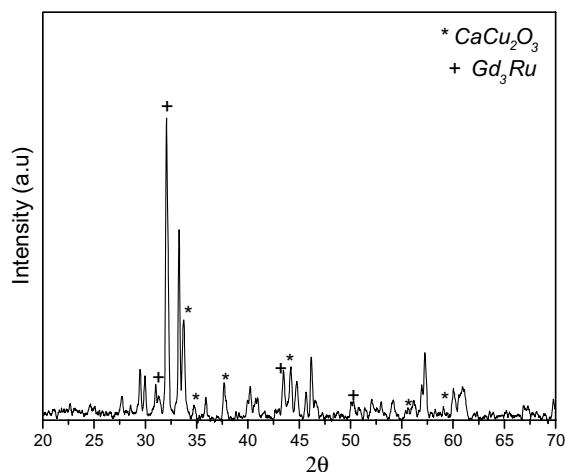


Fig. 3. XRD for $\text{RuCa}_2\text{GdCu}_2\text{O}_8$ compound.

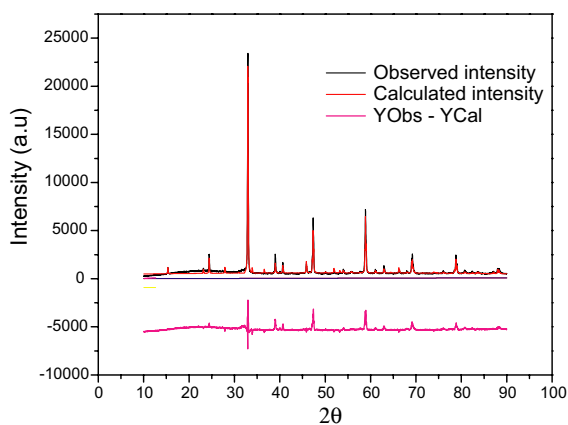


Fig. 4. Observed calculated and difference XRD patterns of $\text{Ru}(\text{Sr}_{1.9}\text{Ca}_{0.1})\text{GdCu}_2\text{O}_8$ composition.

is shown. Different grain sizes that vary between 1 and 6 μm can be observed.

By EDX, a general and dot analysis, in the $\text{Ru}(\text{Sr}_{1.9}\text{Ca}_{0.1})\text{GdCu}_2\text{O}_8$ composition, annealing for 12 h in oxygen flux was carried out. In Fig. 6 the spots labeled A and B, indicate the dot analysis. The results of the chemical compositions are shown in Table 1. The error range of the analysis is between 1 and 6 wt% [16]; therefore it can be said that the experimental and theoretical atomic percentages of the elements resemble each other.

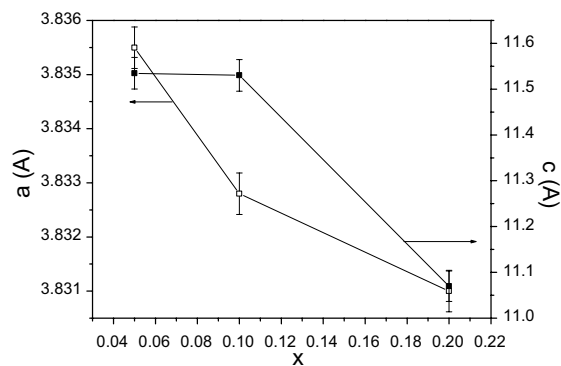


Fig. 5. Variation of lattice parameters a and c of the $\text{Ru}(\text{Sr}_{2-x}\text{Ca}_x)\text{GdCu}_2\text{O}_8$ system.

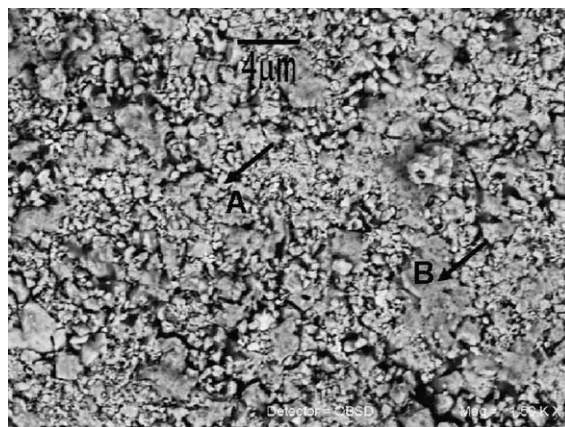


Fig. 6. SEM of $\text{Ru}(\text{Sr}_{1.9}\text{Ca}_{0.1})\text{GdCu}_2\text{O}_8$ composition. The arrows indicate spots for further EDX analysis.

Table 1
EDX analysis of $\text{Ru}(\text{Sr}_{1.9}\text{Ca}_{0.1})\text{GdCu}_2\text{O}_8$ composition

| Elements | Ru | Sr | Ca | Gd | Cu |
|------------------------|-------|-------|------|-------|-------|
| Theoretical percentage | 16.66 | 33.33 | 1.66 | 16.66 | 31.66 |
| General analysis | 16.47 | 33.99 | 1.42 | 18.49 | 29.49 |
| Spot A | 15.86 | 34.16 | 1.34 | 17.58 | 31.06 |
| Spot B | 13.42 | 27.60 | 1.12 | 21.08 | 36.78 |

The single phase of the $\text{Ru}(\text{Sr}_{2-x}\text{Ca}_x)\text{GdCu}_2\text{O}_8$ system, with $x = 0.05$ and 0.1 were characterized using the TEM technique. In Fig. 7 we present



Fig. 7. TEM of the $\text{Ru}(\text{Sr}_{1.9}\text{Ca}_{0.1})\text{GdCu}_2\text{O}_8$ compound.

the electron diffraction patterns of $\text{Ru}(\text{Sr}_{1.9}\text{Ca}_{0.1})\text{GdCu}_2\text{O}_8$ compound in which the tetragonal unit cell was tested.

The lattice parameters were calculated using the formula $\lambda L/R = d_{hkl}$ [16], where L is the variable distance between the specimen and the analyzing crystal = 100 cm, λ is the wavelength of the incident ray beam = 0.4 Å, R is the distance between the center and the different spots and d_{hkl} is the space between the planes in the atomic lattice. The lattice parameters were $a = 3.81$ Å and $c = 11.43$ Å. Therefore, the value of a is similar to that obtained by XRD method, whereas for c it is different. This small difference is probably due to the TEM pattern which was carried out for a monocrystal, while the parameters cell obtained by XRD technique are the average of all crystals.

Fig. 8 shows the temperature dependence of the resistivity on the $\text{Ru}(\text{Sr}_{2-x}\text{Ca}_x)\text{GdCu}_2\text{O}_{8\pm z}$ system with $x = 0.0, 0.05$ and 0.1 , annealed in oxygen flux for 12 h at 960 °C. The curves for $x = 0.05$ and 0.1 show a semiconducting behavior, the $x = 0.0$ data, however, shows a transition in its curvature around 40 K. For all these curves, no superconductivity could be observed under the sample preparation conditions described above. We note that Ca doping considerably reduces the resistance. To explain this phenomenon, substitution of Ca at the Sr site, supposedly changes the electronic structure of Cu–O and Ru–O bond lengths.

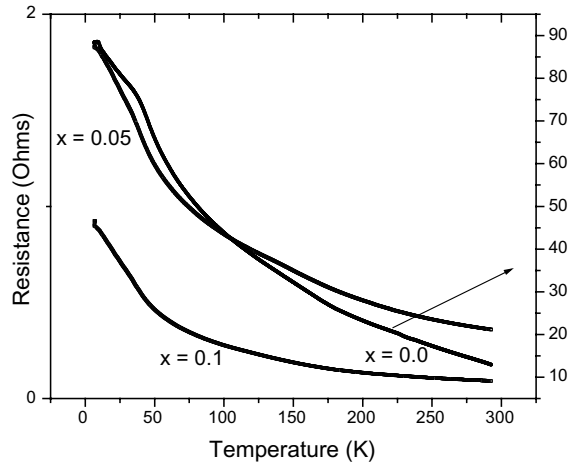


Fig. 8. R vs. T for $\text{Ru}(\text{Sr}_{2-x}\text{Ca}_x)\text{GdCu}_2\text{O}_8$ system.

To verify this probability, a structural refinement by the Rietveld method was carried out using a FullProf program [13] with the starting model previously reported for the Ru-1212 [17]. The O(1) atoms, which are the apical oxygen atoms of the CuO_5 square pyramid, are closed to the Sr site and therefore are most affected by Ca substitution. Rietveld refinement results show that the Cu–O(1) bond lengths in $\text{Ru}(\text{Sr}_{2-x}\text{Ca}_x)\text{GdCu}_2\text{O}_8$ system with $x = 0.00, 0.05$ and 0.10 are 3.8705, 2.2275 and 1.9211 Å, respectively. We note that both Cu–O(1) bond lengths and the resistance on the $\text{Ru}(\text{Sr}_{2-x}\text{Ca}_x)\text{GdCu}_2\text{O}_8$ system decrease with x values.

The samples with $x = 0.0, 0.05, 0.1$ and 0.2 were annealed in oxygen flux at 960 °C for 41 h. Fig. 9 shows the results of the temperature dependence of the resistance. We observed that all samples present a semiconducting behavior. We noted that with an additional annealing in oxygen flux (41 h), the resistance values are 5–92 times smaller as compared to the resistances at 291 K obtained for the samples with $x = 0.0, 0.05$ and 0.1 annealing in oxygen flux for 12 h.

Various groups synthesized $\text{RuSr}_2\text{GdCu}_2\text{O}_8$ samples whose properties varied from superconducting [8,11,18–28] to semiconducting [29,30] depending on the preparation procedure. In general, the superconducting Ru-1212 samples were synthesized by the following conditions: in air,

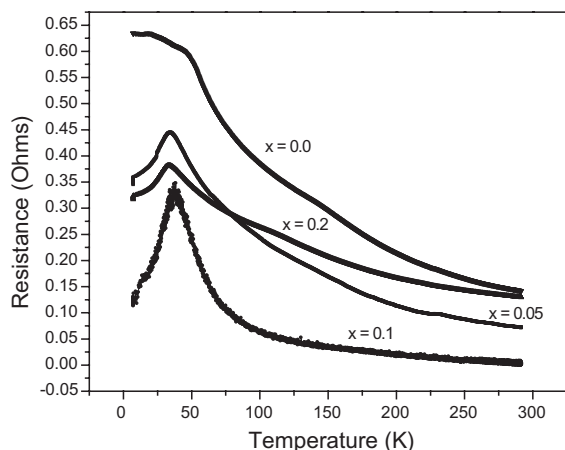


Fig. 9. R vs. T for $\text{Ru}(\text{Sr}_{2-x}\text{Ca}_x)\text{GdCu}_2\text{O}_{8\pm z}$ system.

$T = 600\text{--}1060$ °C for 10–96 h, and in oxygen flux with $T = 1015\text{--}1085$ °C for 10 h–14 d. It was proposed that the annealing at high temperature with long-time (14 d) in oxygen flux is essential for achieving SC. The semiconducting Ru-1212 samples were obtained at $T = 950\text{--}1000$ °C in air, for 1 d and at $T = 1060$ °C in oxygen flux for 72 h [29,30].

From all these studies [8,11,18–30], we noted that the temperatures of annealing in oxygen flux are higher than 960 °C. By TG measurements, we observed that the sample with $x = 0.0$ loses oxygen up to 960 °C, to avoid it, all samples were oxygenated at 960 °C. We consider that our route of synthesis did not give superconductive samples although they are a high-purity phases ($x = 0.0, 0.05$ and 0.1) as shown in Fig. 1.

The results of the DC susceptibility magnetic measurements show that the Sr^{2+} by Ca^{2+} ions did not change the magnetic properties, and on the other hand we did not observe any superconducting phase, that signify a very poor grain–grain.

4. Conclusions

By solid-state reaction at ambient pressure a complete solubility up to $x = 0.1$ was obtained in the $\text{Ru}(\text{Sr}_{2-x}\text{Ca}_x)\text{GdCu}_2\text{O}_8$ system. The compounds with $0.0 < x < 0.2$ exhibit semiconductor behavior.

Acknowledgements

Financial support for this research was provided by CONACyT 33630E, 3427 P, E9607 and P41226F and UNAM DGAPA IN106600 and IX108104. We thank C. Flores, J. Guzmán and C. Vázquez for their technical support.

References

- [1] L. Bauernfeind, W. Widder, H.F. Braun, *Physica C* 254 (1995) 151.
- [2] L. Bauernfeind, W. Widder, H.F. Braun, *J. Low Temp. Phys.* 105 (1996) 1605.
- [3] F. Bobba, F. Giubileo, M. Gombos, C. Noce, A. Vecchione, A.M. Cucolo, D. Roditchev, A. Lamy, W. Sacks, *Int. J. Mod. Phys. B* 17 (4–6) (2003) 608.
- [4] I. Felner, U. Asaf, Y. Levi, O. Millo, *Phys. Rev. B* 55 (1997) R3374.
- [5] B. Lorenz, R.L. Meng, J. Cmaidalka, Y.S. Wang, J. Lenzi, Y.Y. Xue, C.W. Chu, *Physica C* 363 (2001) 251.
- [6] J.L. Tallon, C. Bernhard, M. Bowden, P. Gilber, T. Stoto, D. Pringle, *IEEE T. Appl. Supercond.* 9 (1999) 1696.
- [7] C. Bernhard, J.L. Tallon, Ch. Niedermayer, Th. Blasius, A. Golnik, E. Brucher, R.K. Kremer, D.R. Noajes, C.E. Sronach, E.J. Ansaldo, *Phys. Rev. B* 59 (1999) 14099.
- [8] A.C. McLaughlin, J.P. Attfield, *Phys. Rev. B* 60 (1999) 14605.
- [9] P.B. Klamut, B. Dabrowski, S.M. Mini, M. Maxwell, S. Kolesnik, J. Mais, A. Shengelaya, R. Khasanov, I. Savic, H. Keller, *Physica C* 350 (2001) 24.
- [10] L.T. Yang, J.K. Liang, Q.L. Liu, J. Luo, G.B. Song, F.S. Liu, X.M. Feng, G.H. Rao, *J. Appl. Phys.* 95 (2004) 4.
- [11] P. Mandal, A. Hassen, J. Hemberger, A. Krimmel, A. Loidl, *Phys. Rev. B* 65 (2002) 14506.
- [12] A. Hassen, J. Hemberger, A. Loidl, A. Krimmel, *Physica C* 400 (2003) 70.
- [13] Available from: <http://www.llb.cea.fr/fullweb/fp2k/fp2k_links.htm>.
- [14] V. G-Vázquez, N. Pérez-Amaro, A. Canizo-Cabrera, B. Cumplido-Espíndola, R. Martínez-Hernández, M.A. Abarca-Ramírez, *Rev. Sci. Instrum.* 72 (2001) 3332.
- [15] R.D. Shannon, *Acta Crystallogr. A* 32 (1976) 751.
- [16] D.R. Beaman, J.A. Isasi, *Electron Beam Microanalysis, Special Technical Publication American Society for Testing and Materials* 506 (1972) 23.
- [17] G.M. Kuźmicheva, V.V. Luparev, E.P. Khlybov, I.E. Kostyleva, A.S. Andreenko, K.N. Gavrilov, *Physica C* 350 (2001) 105.
- [18] A. Fainstein, E. Winkler, A. Butera, J. Tallon, *Phys. Rev. B* 60 (1999) R12596.
- [19] J.E. McCrone, J.R. Copper, J.L. Tallon, *J. Low Temp. Phys.* 117 (1999) 1199.

- [20] J.L. Tallon, J.W. Loram, G.V.M. Williams, C. Bernhard, *Phys. Rev. B* 61 (2000) 6471.
- [21] C. Bernhard, J.L. Tallon, E. Brücher, R.K. Kremer, *Phys. Rev. B* 61 (2000) R14960.
- [22] D.Z. Wang, H.I. Ha, J.I. Oh, J. Moser, J.G. Wen, M.J. Naughton, Z.F. Ren, *Physica C* 384 (2003) 137.
- [23] T.P. Papageorgiou, T. Herrmannsdörfer, R. Dinnebier, T. Mai, T. Ernst, M. Wunschel, H.F. Braun, *Physica C* 377 (2002) 383.
- [24] C. Artini, M.M. Carnasciali, G.A. Costa, M. Ferretti, M.R. Cimberle, M. Putti, R. Masini, *Physica C* 377 (2002) 431.
- [25] R.S. Liu, L.Y. Jang, H.H. Hung, J.L. Tallon, *Phys. Rev. B* 63 (2001) 212507.
- [26] A.M. Saleh, M.M. Abu-Samreh, A.A. Leghrouz, *Physica C* 384 (2003) 383.
- [27] H.F. Braun, T.P. Papageorgiou, T. Herrmannsdörfer, L. Baurneind, O. Korf, *Physica C* 387 (2003) 26.
- [28] B. Lorenz, R.L. Meng, Y.Y. Xue, C.W. Chu, *Physica C* 383 (2003) 337.
- [29] I. Felner, U. Asaf, S. Reich, Y. Tsabba, *Physica C* 311 (1999) 163.
- [30] M. Li, M. Yu, Z. Wang, H. Yang, Y. Hu, Z. Chen, Z. Li, L. Cao, *Physica C* 382 (2002) 233.